

A Model for Simulating the Performance of a Shallow Pond as a Supplemental Heat Rejecter with Closed-Loop Ground-Source Heat Pump Systems

Andrew D. Chiasson
Student Member ASHRAE

Jeffrey D. Spitler, Ph.D., P.E.
Member ASHRAE

Simon J. Rees, Ph.D.
Member ASHRAE

Marvin D. Smith, P.E.

ABSTRACT

Commercial buildings and institutions are generally cooling-dominated and therefore reject more heat to a ground-loop heat exchanger than they extract over the annual cycle. This paper describes the development, validation, and use of a design and simulation tool for modeling the performance of a shallow pond as a supplemental heat rejecter in ground-source heat pump systems. The model has been developed in the TRNSYS modeling environment and can therefore be coupled to other GSHP system component models for short time step (hourly or less) system analyses. The model has been validated by comparing simulation results to experimental data collected from two test ponds. The solution scheme involves a lumped-capacitance approach, and the resulting first-order differential equation describing the overall energy balance on the pond is solved numerically. An example application is presented to demonstrate the use of the model as well as the viability of the use of shallow ponds as supplemental heat rejecters in GSHP systems. Through this example, it is shown that ground-loop heat exchanger size can be significantly decreased by incorporating a shallow pond into a GSHP system.

INTRODUCTION

Ground-source heat pump (GSHP) systems have become increasingly popular for both residential and commercial heating and cooling applications because of their higher energy efficiency compared to conventional systems. In closed-loop GSHPs, heat rejection/extraction is accomplished by circulating a heat exchange fluid (water or antifreeze) through high-density polyethylene pipe buried in horizontal trenches or vertical boreholes. In large-scale commercial applications,

vertical borehole systems are preferred over horizontal trench systems because less ground area is required.

Commercial buildings and institutions are generally cooling-dominated and therefore reject more heat than they extract over the annual cycle. In order to adequately dissipate the imbalanced annual loads, the required ground-loop heat exchanger lengths are significantly greater than the required length if the annual loads were balanced. Consequently, under these circumstances, ground-source heat pump systems may be eliminated from consideration during the feasibility study phase of the HVAC design process because of excessive first cost.

To effectively balance the ground loads and reduce the necessary size of the ground-loop heat exchanger, supplemental components can be integrated into the ground-loop heat exchanger design. GSHP systems that incorporate some type of supplemental heat rejecter are commonly referred to as hybrid GSHP systems. In applications where the excess heat that would otherwise build up in the ground is useful, domestic hot water heaters, car washes, and pavement heating systems can be used. In cases where the excess heat cannot be used beneficially, shallow ponds can provide a cost-effective means to balance the thermal loading to the ground and reduce heat exchanger length.

The objective of this work has been to develop a design and simulation tool for modeling the performance of a shallow pond that can be usefully and cost-effectively integrated into a ground-source heat pump system as a supplemental heat rejecter. The pond model has been developed in the TRNSYS modeling environment (SEL 1997) and can be coupled to other GSHP system component models for short time step (hourly or less) system analyses. The model has been vali-

Andrew D. Chiasson is a research assistant, **Jeffrey D. Spitler** is a professor, and **Simon J. Rees** is a visiting assistant professor in the School of Mechanical and Aerospace Engineering at Oklahoma State University, Stillwater. **Marvin D. Smith** is a professor in the Division of Engineering Technology at Oklahoma State University.

dated by comparing simulation results to experimental data. As an example of the model's applicability, GSHP system simulation results are presented for a commercial building located in Tulsa, Oklahoma, with a hypothetical closed-loop GSHP system with and without a shallow pond supplemental heat rejecter.

HEAT TRANSFER IN PONDS

General Overview

Pertinent concepts of heat transfer in ponds and lakes have been summarized by many sources. Dake and Harleman (1969) conducted studies of thermal stratification in lakes and addressed the overall thermal energy distribution in lakes. ASHRAE (1995a, 1995b) and Kavanaugh and Rafferty (1997) describe heat transfer in lakes in relation to their use as heat sources and sinks.

Solar energy is identified as the main heating mechanism for ponds and lakes. The main cooling mechanism is evaporation. Thermal radiation can also account for a significant amount of cooling during night hours. Convective heating or cooling to the atmosphere is less significant. Natural convection of water due to buoyancy effects is the primary mechanism for heat transfer within a surface water body. Conductive heat transfer to the ground is generally a relatively insignificant process, except in cases where the water surface is frozen.

Shallow ponds are generally thermally unstratified. Natural stratification of deeper ponds and lakes is due to buoyancy forces and to the fact that water is at its greatest density at 39.2°F (4°C). Therefore, over the annual cycle, water in deeper ponds will completely overturn. Thermal stratification in ponds is also dictated by inflow and outflow rates or groundwater seepage rates. If inflow and outflow rates are high enough, the pond will not stratify. Consequently, thermal stratification occurs only in ponds and lakes that are relatively deep, generally greater than 20-30 ft (6.1-9.1 m), with low

inflow rates. The relevant heat transfer mechanisms occurring within shallow ponds are illustrated in Figure 1.

Existing Pond and Lake Models

Several mathematical and computer models have been developed for simulation of lakes used as heat sinks/sources and for solar ponds.

Raphael (1962) developed a numerical model for determining the temperature of surface water bodies as heat sinks for power plants. Thermal stratification of the water body was not considered. Input data to the model included weather data and inflow and outflow data for the water body. Raphael reported that the model successfully predicted the temperature changes in a river used as a heat sink for a power plant.

Jobson (1973) developed a mathematical model for water bodies used as heat sinks for power plants. Thermal stratification of the water body was not considered. The results of that work showed that the heat transfer at the water/air interface is highly dependent on the natural water temperature and the wind speed.

Cantrell and Wepfer (1984) developed a numerical model for evaluating the potential of shallow ponds for dissipating heat from buildings. The model takes weather data and building cooling load data as inputs and computes the steady-state pond temperature using an energy balance method. Thermal stratification of the pond was not considered. The model showed that a 3 acre (12,141 m²), 10 ft (3.048 m) deep pond in Cleveland, Ohio, could reject 1000 tons (3516 kW) of thermal energy with a maximum increase in pond temperature of about 5°F (2.78°C) over a daily cycle.

Rubin et al. (1984) developed a model for solar ponds. The purpose of a solar pond is to concentrate heat energy from the sun at the pond bottom. This is accomplished by suppressing natural convection within the pond induced by bottom heating, usually by adding a brine layer at the pond bottom. As

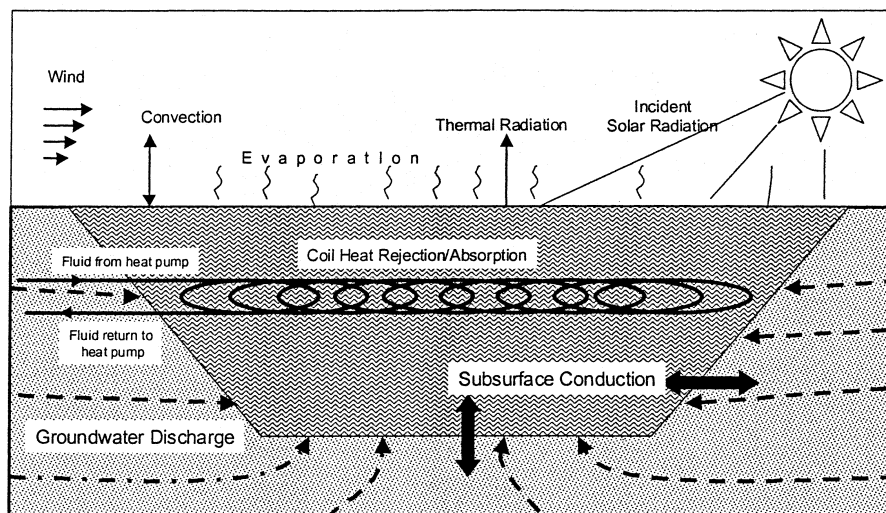


Figure 1 Heat transfer mechanisms in shallow ponds.

a result, solar ponds have three distinct zones as described by Newell (1984):

1. a top layer that is stagnated by some method and acts as a transparent layer of insulation,
2. a middle layer that is usually allowed to be mixed by natural convection, and
3. a lower layer where solar energy is collected.

The model of Rubin et al. (1984) applied an implicit finite difference scheme to solve a one-dimensional heat balance equation on a solar pond. Large-scale convective currents in the pond were assumed to be negligible while small-scale convective currents were handled by allowing the coefficient of heat diffusion to vary through the pond depth. Solar radiation was modeled as an exponentially decaying function through the pond depth. The model successfully predicted seasonal variations in solar pond temperatures.

Srinivasan and Guha (1987) developed a model similar to the model of Rubin et al. (1984) for solar ponds. The Srinivasan and Guha (1987) model consisted of three coupled differential equations, each describing a thermal zone within the solar pond. Solar radiation in each zone is computed as a function of depth. The model also successfully predicted seasonal variations in solar pond temperatures with various heat extraction rates.

Pezent and Kavanaugh (1990) developed a model for lakes used as heat sources or sinks with water-source heat pumps. The model essentially combined the models of Srinivasan and Guha (1987) to handle stratified cases and of Raphael (1962) to handle unstratified cases. As such, thermal

stratification of a lake could be handled in the summer months when lakes are generally most stratified and neglected in the winter months when lakes are generally unstratified. The model is driven by monthly average bin weather data and handles both heat extraction and heat rejection. With no heat extraction or rejection, the model favorably predicted a lake temperature profile in Alabama. The temperatures within the upper zone of the lake (the epilimnion) and the lower zone of the lake (the hypolimnion) were predicted to within 4°F (2.22°C) and approximately 1°F (0.55°C), respectively. However, the model had some difficulty in matching the intermediate zone (the thermocline), perhaps due to the fact that this zone possesses moving boundaries (unlike the boundaries of a solar pond, which are more distinct). As concluded by Pezent and Kavanaugh (1990), a numerical method is necessary to more accurately predict the thermocline profile.

The model presented in this paper is based on the assumption that thermal gradients in shallow ponds are small, especially during times of heat rejection. This model is developed in the TRNSYS modeling environment and can be coupled to other component models for larger system simulations. Furthermore, this model allows the pond performance to be simulated on hourly or less time scales.

EXPERIMENTAL METHODS

Pond Description and Data Collection

Two ponds were constructed for this study on a test site at an Oklahoma university. The layout of the experimental ponds is shown in Figure 2. The ponds are rectangular with a

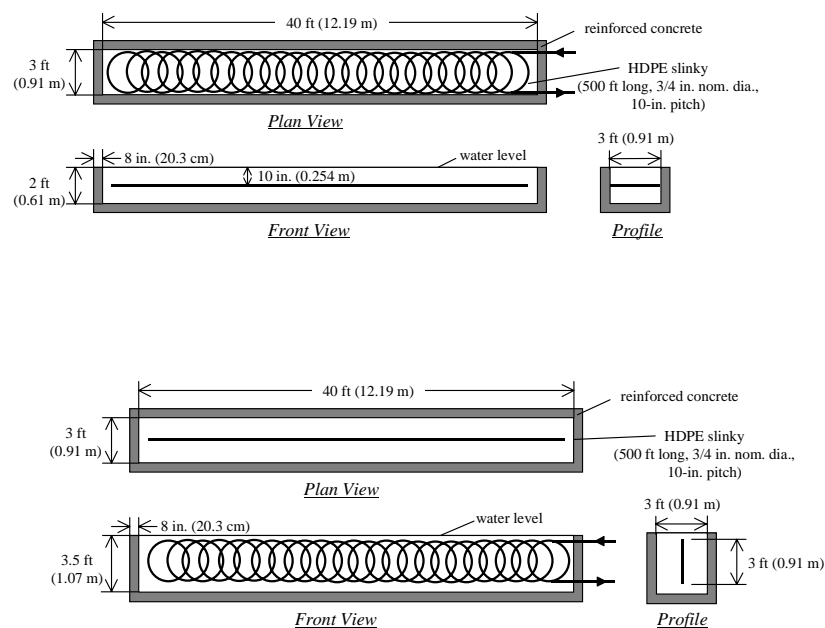


Figure 2 Layout of the shallow experimental ponds showing (a) the horizontally positioned slinky and (b) the vertically positioned slinky.

plan area of 40 ft (12.19 m) by 3 ft (0.91 m). Each pond was constructed with vertical sidewalls, with one of the ponds being 2 ft (0.61 m) deep and the other being 3.5 ft (1.07 m) deep. The walls and the bottom of each pond were constructed of reinforced concrete, approximately 8 in. (20.3 cm) thick.

Heat was rejected to each pond by circulating heated water through a “slinky” heat exchanger (a pipe coiled in a circular fashion such that each loop overlaps the adjacent loop) installed in each pond. Each slinky pipe was made of high-density polyethylene plastic and is 500 ft (152.40 m) long with a nominal diameter of 3/4 in. (0.019 m). The pipe was coiled so that the resulting slinky heat exchanger was 40 ft (12.19 m) long with a diameter of 3 ft (0.91 m) and a 10 in. (0.254 m) pitch (the separation distance between the apex of each successive loop). In the 2 ft (0.61 m) deep pond, the slinky heat exchanger was positioned horizontally within the pond at a depth of approximately 10 in. (0.254 m). In the 3.5 ft (1.07 m) deep pond, the slinky heat exchanger was positioned vertically within the pond along the centerline of the long axis of the pond.

The temperature of the pond water was measured by thermistors positioned at four locations within the pond: (1) near the pond surface at the center of the slinky, (2) below the slinky at its center, (3) near the pond surface at the end opposite from the supply end, and (4) below the slinky at the end of the pond opposite from the supply end. Slinky supply and return water temperatures were measured by thermistors embedded in the slinky header. Each system also included a flow meter, a water heating element, and a watt transducer. All sensor information was recorded by the data acquisition system at time intervals of six minutes.

The tests were controlled to maintain a set supply water temperature by heating the supply water if the temperature fell below a set point. Two set point temperatures were used in this study, 9°F (32.2°C) in the summer season and 75°F (23.9°C) in the winter season.

Weather Instrumentation and Data Collection

Weather data for this study were obtained from the Oklahoma Mesonet (**mesoscale network**), which is a weather station network consisting of weather monitoring sites scattered throughout Oklahoma. Depending on the weather parameter, data are recorded at time intervals ranging from 3 to 30 seconds and averaged over five-minute observation intervals.

Weather data at 15-minute intervals for the Stillwater monitoring station were acquired for the time periods of interest for this study. The Stillwater station is located approximately one mile from the test pond site. Data for the following parameters were obtained: wind speed, wind direction, air temperature, relative humidity, and solar radiation. Further details of the weather station network may be found in Elliott et al. (1994).

MODEL DEVELOPMENT

Governing Equations

The governing equation of the model is an overall energy balance on the pond using the lumped capacitance (or lumped parameter) approach,

$$q_{in} - q_{out} = V\rho c_p \frac{dT}{dt}, \quad (1)$$

where q_{in} is the heat transfer to the pond, q_{out} is the heat transfer from the pond, V is the pond volume, ρ is the density of the pond water, c_p is the specific heat capacity of the pond water, and $\frac{dT}{dt}$ is the rate of change of temperature of the pond water. This approach assumes that temperature gradients within the water body can be neglected. Considering the heat transfer mechanisms shown in Figure 1, Equation 1 can be expressed to describe the rate of change in average pond temperature as

$$\frac{dT}{dt} = (q_{solar} + q_{thermal} + q_{convection} + q_{ground} + q_{groundwater} + q_{evaporation} + q_{fluid}) / V\rho c_p, \quad (2)$$

where

- q_{solar} = solar radiant heat gain to the pond,
- $q_{thermal}$ = thermal radiant heat transfer at the pond surface,
- $q_{convection}$ = convective heat transfer at the pond surface,
- q_{ground} = heat transfer to/from the ground in contact with the pond,
- $q_{groundwater}$ = heat transfer due to groundwater inflow or outflow,
- $q_{evaporation}$ = heat/mass transfer due to evaporation at the pond surface,
- q_{fluid} = total heat transfer to/from the heat exchange fluid flowing in all spools or coils in the pond.

Each of the heat transfer terms used in the above equation is defined briefly below. Further details can be found in Chiasson (1999).

Solar Radiant Heat Gain

Solar radiant heat gain (q_{solar}) is the net solar radiation absorbed by the pond. It is assumed that all solar radiation incident on the pond surface becomes heat gain except for the portion reflected at the surface.

To determine the reflected component of solar radiation, the angle of incidence (θ) of the sun’s rays is first computed at each time step from equations given by Spencer (1971), Duffie and Beckman (1991), and ASHRAE (1997). The angle of refraction of the sun’s rays at the pond surface is determined by Snell’s law. The reflectance (ρ^{\prime}) is then computed after Duffie and Beckman (1991). The amount of solar radiation absorbed by the pond (q_{solar}) is expressed as

$$q_{solar} = I(1 - \rho^{\prime})A_{pond}, \quad (3)$$

where I is the solar radiant flux incident on the pond surface

(here, the total reflectance is approximated by the beam reflectance) and A_{pond} is the area of the pond surface. The model also accepts solar radiation in the form of beam (I_b) and diffuse (I_d) components, in which case I is computed from

$$I = I_b \cos\theta + I_d. \quad (4)$$

Thermal Radiant Heat Transfer

This heat transfer mechanism accounts for heat transfer at the pond surface due to thermal or long-wave radiation. This model uses a linearized radiation coefficient (h_r) defined as

$$h_r = 4\epsilon\sigma\left(\frac{T_{pond} + T_{sky}}{2}\right)^3 \quad (5)$$

where ϵ is the emissivity coefficient of the pond water, σ is the Stefan-Boltzmann constant, T_{pond} is the pond temperature in absolute units, and T_{sky} is the sky temperature in absolute units. T_{sky} is computed from a relationship given by Bliss (1961). The thermal radiant heat transfer ($q_{thermal}$) is then computed by

$$q_{thermal} = h_r A_{pond} (T_{sky} - T_{pond}). \quad (6)$$

Convective Heat Transfer at the Pond Surface

This mechanism accounts for heat transfer at the pond surface due to free and forced convection. Several empirical formulations exist for determining the convection coefficient for different geometries. For a pond surface, correlations for a horizontal flat plate are the most applicable.

In free convection heat transfer, the Nusselt number (Nu) is often correlated to the Rayleigh number (Ra). In external free convection flows over a horizontal flat plate, the critical Rayleigh Number is about 10^7 . Therefore, two empirical relations for the Nusselt number are used in the model as described by Incropera and DeWitt (1996) for free convection from the upper surface of a heated plate or the lower surface of a cooled plate:

$$Nu = 0.54Ra^{1/4} \quad (10^4 < Ra < 10^7 - \text{laminar flow}) \quad (7a)$$

$$Nu = 0.15Ra^{1/3} \quad (10^7 > Ra > 10^{11} - \text{turbulent flow}) \quad (7b)$$

The convection coefficient (h_c) for free convection can then be determined from

$$h_c = \frac{Nu k}{L} \quad (8)$$

where k is the thermal conductivity of air evaluated at the film temperature (as with the other thermal properties of air) and L is the characteristic length described for horizontal flat plates as the ratio of the area to the perimeter (Incropera and DeWitt 1996).

In forced convection heat transfer, Nu is a function of the Reynolds (Re) and Prandtl (Pr) numbers. For external forced convection over a flat plate (i.e., the pond surface), the critical Reynolds number is approximately 10^5 (Incropera and DeWitt

1996). Therefore, two empirical relations for the Nusselt number are used in the model as described by Incropera and DeWitt (1996) for forced convection over a flat plate:

$$Nu = 0.664Re^{1/2}Pr^{1/3} \quad (\text{laminar flow regime}) \quad (9a)$$

$$Nu = 0.037Re^{4/5}Pr^{1/3} \quad (\text{mixed and turbulent flow}) \quad (9b)$$

The convection coefficient (h_c) for forced convection can then be determined by Equation 8 with the characteristic length value described as the ratio of the length (parallel to the wind direction) to the perimeter.

Finally, the convective heat transfer at the pond surface ($q_{convection}$) is computed by

$$q_{convection} = h_c A_{pond} (T_{air} - T_{pond}) \quad (10)$$

where T_{air} is the ambient air temperature and h_c is taken as the maximum of the free convection coefficient and the forced convection coefficient. This practice of choosing the larger of the free and forced convection coefficients is recommended by Duffie and Beckman (1991) and McAdams (1954) and is used in the absence of additional experimental evidence regarding combined free and forced convection.

Heat Transfer to the Ground

This heat transfer mechanism accounts for heat conduction to/from the soil or rock in contact with the sides and the bottom of the pond. This mechanism of heat transfer is highly site-specific and complex and depends on many factors, such as soil/rock thermal properties, climatic factors, pond geometry, and thermal loading history. In this model, we chose to use a semi-empirical approach developed by Hull et al. (1984) to determine heat losses/gains from the bottom and sides of the pond. Hull et al. (1984) used a three-dimensional numerical code to compute steady-state ground heat losses from solar ponds of varying sizes, geometries, and sidewall insulation types.

Hull et al. (1984) express ground heat losses from any pond as a function of the pond area, pond perimeter, the ground thermal conductivity (k_{ground}), and the distance from the pond bottom to a constant temperature sink. For practical purposes, the constant temperature sink can be taken as the groundwater table (Kishore and Joshi 1984). For a rectangular pond with vertical side walls, a heat transfer coefficient for ground heat transfer (U_{ground}) can be computed from

$$U_{ground} = 0.999\left(\frac{k_{ground}}{d_{groundwater} - d_{pond}}\right) + 1.37\left(\frac{k_{ground}P_{pond}}{A_{pond}}\right), \quad (11)$$

where k_{ground} is the thermal conductivity of the ground, $d_{groundwater}$ is the depth to the water table or the constant source/sink from the ground surface, d_{pond} is the pond depth, and P_{pond} is the pond perimeter. The conductive heat transfer between the ground and the pond (q_{ground}) is then given by

$$q_{ground} = U_{ground} A_{pond} (T_{groundwater} - T_{pond}). \quad (12)$$

It is recognized that the above conductive heat transfer model is a relatively simple representation of the true transient behavior of heat transfer in the ground. However, ground heat conduction is a relatively minor process affecting the overall heat transfer within the pond as compared to other processes.

Heat Transfer Due to Ground Water Seepage

This heat transfer mechanism accounts for inflows and outflows of groundwater to the pond. Although groundwater contributions may not be expected in shallow heat rejecter ponds, this heat transfer mechanism can be used to account for other inflows and outflows, such as makeup water or rain water.

The volumetric groundwater flow rate (Q) is computed by Darcy's Law:

$$Q = Ki (P_{pond} [d_{pond} - d_{groundwater}] + A_{pond}) \quad (13)$$

where K is the hydraulic conductivity of the soil/rock surrounding the pond and i is the hydraulic gradient. The heat transfer contribution from ground water ($q_{groundwater}$) is then given by

$$q_{groundwater} = Q\rho c_p (T_{groundwater} - T_{pond}) \quad (14)$$

where ρ and c_p represent the density and specific heat capacity of groundwater. These properties of groundwater are computed from relationships given in the *Handbook of Chemistry and Physics* (CRC 1980).

Heat Transfer Due to Evaporation

This heat transfer mechanism is the most important contributing to pond cooling. This model uses the j-factor analogy to compute the mass transfer of evaporating water (\dot{m}_w'') at the pond surface:

$$\dot{m}_w'' = h_d(w_{air} - w_{surf}), \quad (15)$$

where h_d is the mass transfer coefficient, w_{air} is the humidity ratio of the ambient air, and w_{surf} represents the humidity ratio of saturated air at the pond surface. The mass transfer coefficient (h_d) is defined using the Chilton-Colburn analogy as

$$h_d = \frac{h_c}{c_p Le^{2/3}} \quad (16)$$

where h_c is the convection coefficient defined previously, c_p is the specific heat capacity of the air evaluated at the pond-air film temperature, and Le is the Lewis number. Le is computed as

$$Le = \frac{\alpha}{D_{AB}} \quad (17)$$

where α is the thermal diffusivity of the air and D_{AB} represents the binary diffusion coefficient, each evaluated at the pond-air film temperature.

The heat transfer due to evaporation ($q_{evaporation}$) is then computed by

$$q_{evaporation} = h_{fg} A_{pond} \dot{m}_w'' \quad (18)$$

where h_{fg} is the latent heat of vaporization and is computed at each time step from the relationship given by Irvine and Liley (1984).

Heat Transfer Due to the Heat Exchange Fluid

Heat transfer due to the heat exchange fluid represents the pond thermal load. This model has been developed to account for water or antifreeze as the heat exchange fluid. The thermal properties of the fluid are computed at each time step from correlations given in the *Handbook of Chemistry and Physics* (CRC 1980) for water and from correlations given by Wadivkar (1997) for an antifreeze solution. The thermal properties are computed at the average fluid temperature (T_{fluid}). This temperature is computed as the average of the inlet and outlet temperatures at the given time step. Since the outlet temperature at any current time step is not known, the previous converged value is used as an initial guess and calculation of T_{fluid} is iterative. Solution of the pond temperature is also an iterative procedure as discussed below.

The heat transfer due to the heat exchange fluid (q_{fluid}) is computed by

$$q_{fluid} = UA_{pipe} (T_{fluid} - T_{pond})(N_{circuit}) \quad (19)$$

where UA_{pipe} is the overall heat transfer coefficient for the pipe expressed in terms of inside pipe area, and $N_{circuit}$ refers to the number of flow circuits (i.e., the number of spools) installed in the pond. Thus, Equation 19 is based on the assumption that one spool is one flow circuit and that the flow rate is divided evenly between the circuits in a parallel arrangement. The term UA_{pipe} is expressed in terms of the inside pipe area as

$$UA_{pipe} = \frac{2\pi r_i L_{spool}}{\Sigma R_t}, \quad (20)$$

where r_i is the inner pipe radius, L_{spool} is the length of one spool or circuit, and ΣR_t represents the composite thermal resistance that is defined by the following resistance network:

$$\Sigma R_t = R_i + R_{pipe} + R_o + ff \quad (21)$$

where R_i is the thermal resistance due to fluid flow through the pipe, R_{pipe} is the pipe thermal resistance, R_o is the thermal resistance at external pipe surface, and ff represents a fouling factor at both the inner and outer pipe walls. The resistance terms are defined as follows (in terms of inner pipe radius):

$$R_i = \frac{1}{h_i}, \quad (22)$$

$$R_{pipe} = \frac{r_i}{k_{pipe}} \ln\left(\frac{r_o}{r_i}\right), \quad (23)$$

and

$$R_o = \frac{r_i}{r_o} \left(\frac{1}{h_o} \right), \quad (24)$$

where h_i is the convection coefficient due to fluid flow through the pipe, k_{pipe} is the thermal conductivity of the pipe material, h_o is the convection coefficient at the outer surface of the pipe, and r_i and r_o are the inner and outer radii of the pipe, respectively.

The above convection coefficients are determined using correlations for the Nusselt number in flow through a horizontal cylinder since no specific correlations exist for a slinky coil. A constant heat flux at the pipe surface is assumed. For laminar, fully developed flow in the pipe ($Re < 2000$), the Nusselt number is a constant equal to 4.36 (Incropera and DeWitt 1996, Equation 8-53). For turbulent flow, the Dittus-Boelter relation is used to compute the Nusselt number:

$$Nu_i = 0.023Re^{4/5}Pr^x. \quad (25)$$

The value of the exponent x in Equation 25 is dependent upon whether the entering fluid is being heated or cooled; $x = 0.3$ if the entering fluid is greater than the pond temperature and $x = 0.4$ if the entering fluid is less than the pond temperature. The convection coefficient for flow inside the pipe (h_i) is given by Equation 8 where Nu is equal to Nu_i , k is the thermal conductivity of the heat transfer fluid, and the characteristic length (L) is the inner diameter of the pipe.

Convection at the external pipe surface is considered to be free convection and is most similar to the case of a horizontal cylinder. The correlation used in the model for free convection from a horizontal cylinder is defined as (Churchill and Chu 1975)

$$Nu_o = \left(0.60 + \frac{0.387Ra^{1/6}}{(1 + (0.559/Pr)^{9/16})^{8/27}} \right)^2. \quad (26)$$

The convection coefficient at the external pipe surface (h_o) is given by Equation 8 where Nu is equal to Nu_o , k is the thermal conductivity of the pond water, and the characteristic length (L) is the outer diameter of the pipe.

The outlet fluid temperature (T_{out}) is computed from an overall energy balance on the pipe:

$$T_{out} = T_{fluid} - \frac{q_{circuit}}{2\dot{m}c_p} \quad (27)$$

where \dot{m} is the mass flow rate of the heat exchange fluid per flow circuit, c_p is the specific heat capacity of the heat exchange fluid, and $q_{circuit}$ is the heat rejected/extracted by one flow circuit. This outlet temperature is used to compute the average fluid temperature at the next iteration as described above.

Solving the Overall Energy Balance Equation

The differential equation describing the overall energy balance on the pond (Equation 2) is rearranged in the following form:

$$\frac{dT}{dt} = x_1T + x_2 \quad (28)$$

where T represents the pond temperature, x_1 contains all terms of Equation 2 that multiply T , and x_2 contains all terms of Equation 2 that are independent of T . Equation 28 is a linear first-order ordinary differential equation that is solved at each time step using the exponential function as an integrating factor.

Many of the quantities in the heat transfer equations described above require that the average pond temperature at the current time step be known. Thus, the actual pond temperature is found iteratively. A convergence criterion for the pond temperature of 1.8×10^{-5} °F (1×10^{-5} °C) is used.

Computer Implementation

The component configuration for the pond model is shown in Figure 3. A companion model was also developed that manipulates any weather data needed for the pond model. The weather component model makes use of the TRNSYS psychrometric subroutine to compute moist air properties given two known state properties. The two state properties are dry-bulb temperature and either wet-bulb temperature, relative humidity, or dew point temperature. The weather component model also computes the sky temperature, the solar radiation on a horizontal surface, and the solar incidence angle. A computer algorithm is shown in Figure 4 in the form of a flow chart.

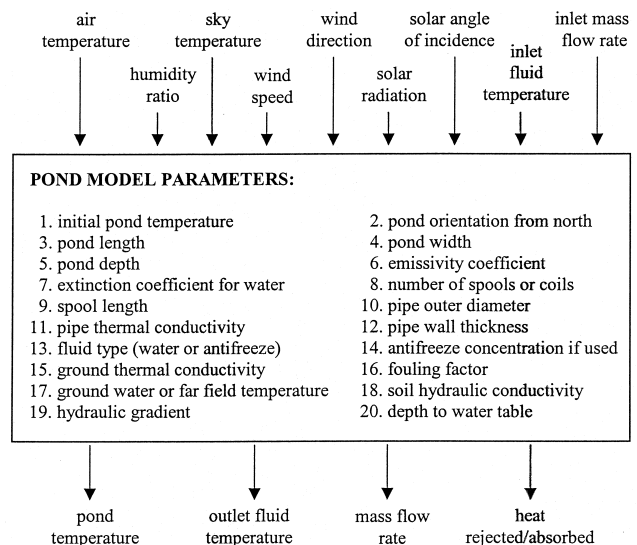


Figure 3 Pond model component configuration.

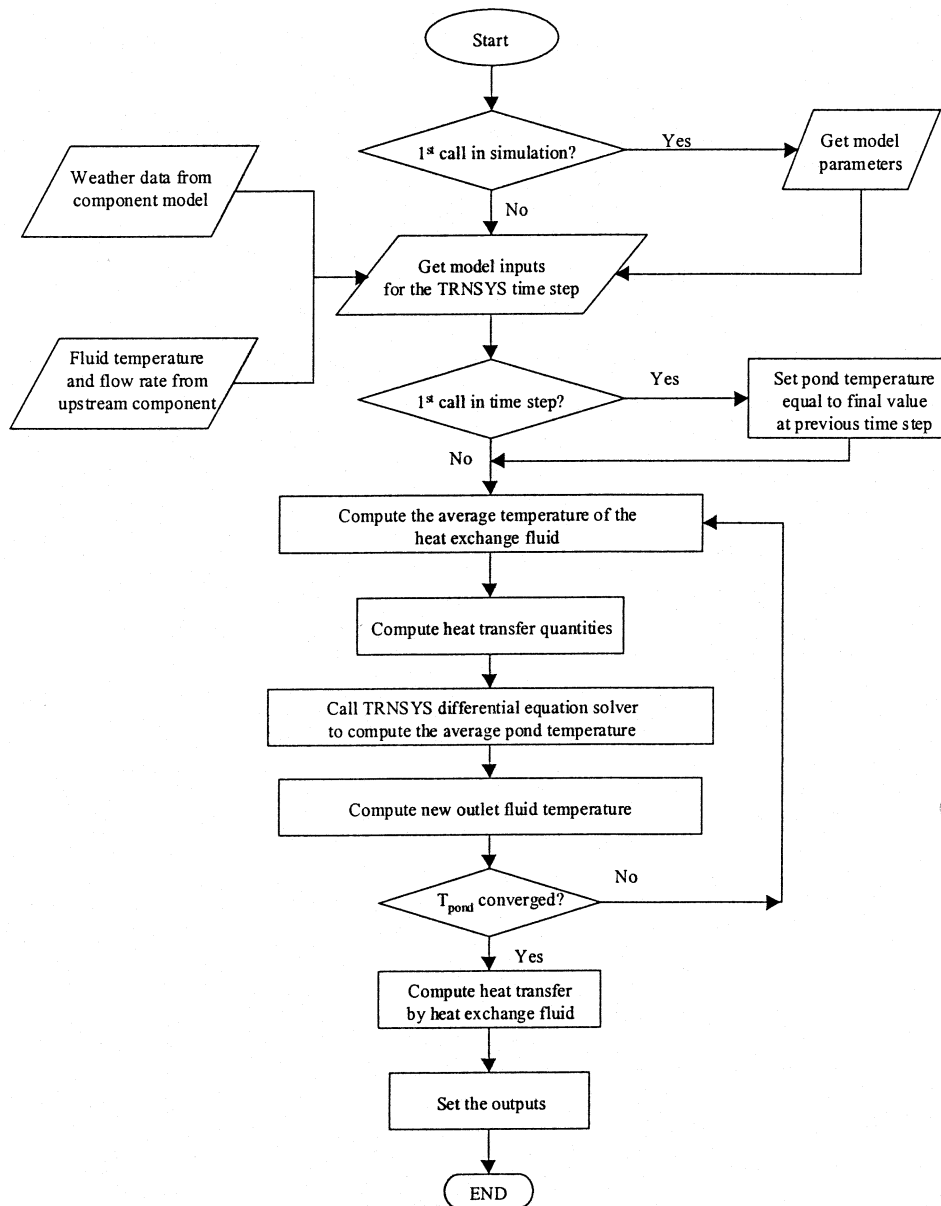


Figure 4 Pond model computer algorithm.

RESULTS AND DISCUSSION

Model Comparison to Experimental Results with No Heat Rejection

The first step in the model verification process was to compare the model pond temperatures to measured pond temperatures during times when no heat was being rejected to the ponds. This comparison allowed a validity check of the simulation of the several environmental heat transfer mechanisms occurring within the ponds, as well as an assessment of the validity of the lumped capacitance approach. Simulated and actual pond average hourly temperatures are shown in

Figure 5 for an eight-day period in July 1998 when no heat was rejected to the ponds. Therefore, in these cases, the model is driven by weather data input only. Shallow groundwater was not encountered at the site, and, therefore, groundwater contributions were not considered.

A review of the plots in Figure 5 shows that the temperature variation within the ponds is relatively small; hence, the lumped parameter approach is appropriate. The temperature variation between the top surface and the bottom of the 2 ft deep pond averaged 1.2°F (0.65°C) for the test period duration, with a maximum difference of 5.6°F (3.1°C) occurring on one occasion. The temperature variation between the top surface

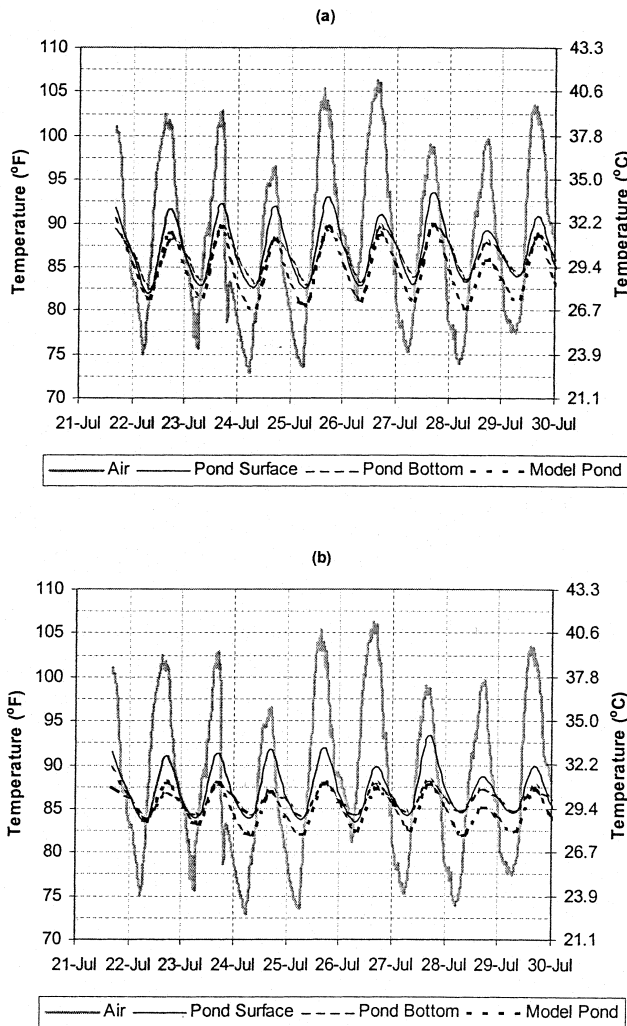


Figure 5 Comparison of observed and simulated average pond temperatures with no heat rejection in the (a) 2 ft (0.61 m) deep pond and (b) 3.5 ft (1.07 m) deep pond.

and the bottom of the 3.5 ft deep pond averaged 1.4°F (0.77°C) for the test period duration, with a maximum difference of 6.0°F (3.3°C) occurring on one occasion.

The model temperatures also compare favorably to the overall average measured pond temperatures. The simulated temperatures are within 3°F (1.67°C) of the observed average pond temperatures throughout the test period. The difference between the average simulated pond temperature and the average observed pond temperature for the entire test period is 1.93°F (1.07°C) for the 2 ft deep pond and 1.55°F (0.86°C) for the 3.5 ft deep pond.

Model Comparison to Experimental Results with Heat Rejection

Heat rejection to the ponds was simulated over a 25-day period from November 12 to December 7, 1998. Input data to

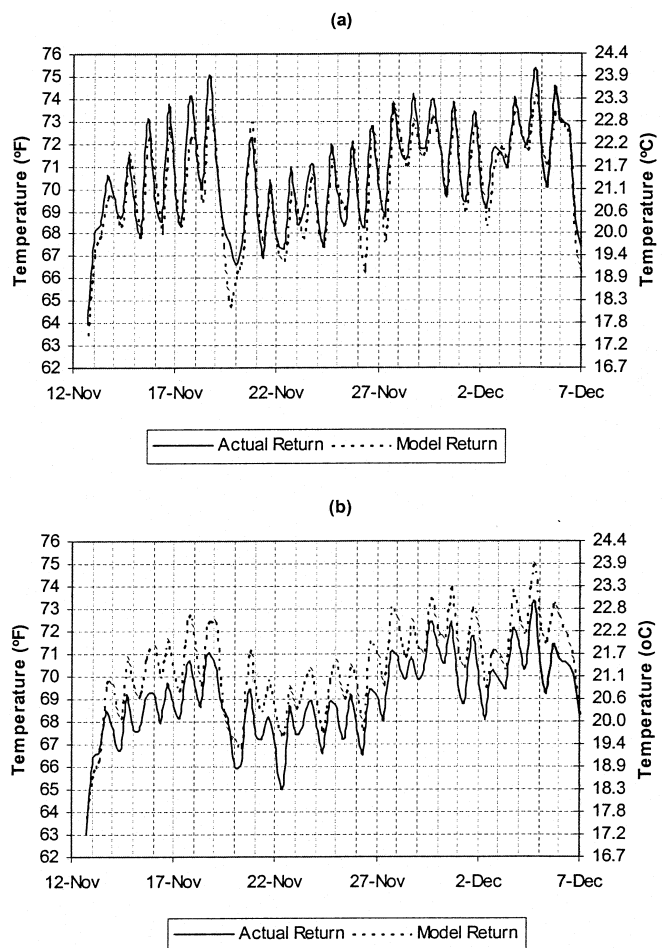


Figure 6 Comparison of observed and simulated heat exchange fluid return temperatures for the (a) 2 ft (0.61 m) deep pond and (b) 3.5 ft (1.07 m) deep pond.

the model consisted of weather data as described previously in addition to measured slinky heat exchanger supply water temperatures and flow rates at six-minute time intervals. The model performance was evaluated by comparing (1) the simulated to the observed return temperature of the heat exchange fluid and (2) the simulated cumulative heat rejected to the ponds to the measured water heating element and pump power input. These comparisons are shown in Figures 6 and 7, respectively. As with the previous comparisons, groundwater contributions and fouling of the heat exchanger pipe were not considered.

A review of the temperature plots in Figure 6 shows that modeled fluid return temperatures compare favorably to the observed fluid return temperatures. The average observed and modeled fluid return temperatures over the test period in the 2 ft (0.61 m) deep pond were 70.5°F (21.4°C) and 70.2°F (21.2°C), respectively, and in the 3.5 ft (1.07 m) deep pond were 69.2°F (20.7°C) and 70.4°F (21.3°C), respectively. The

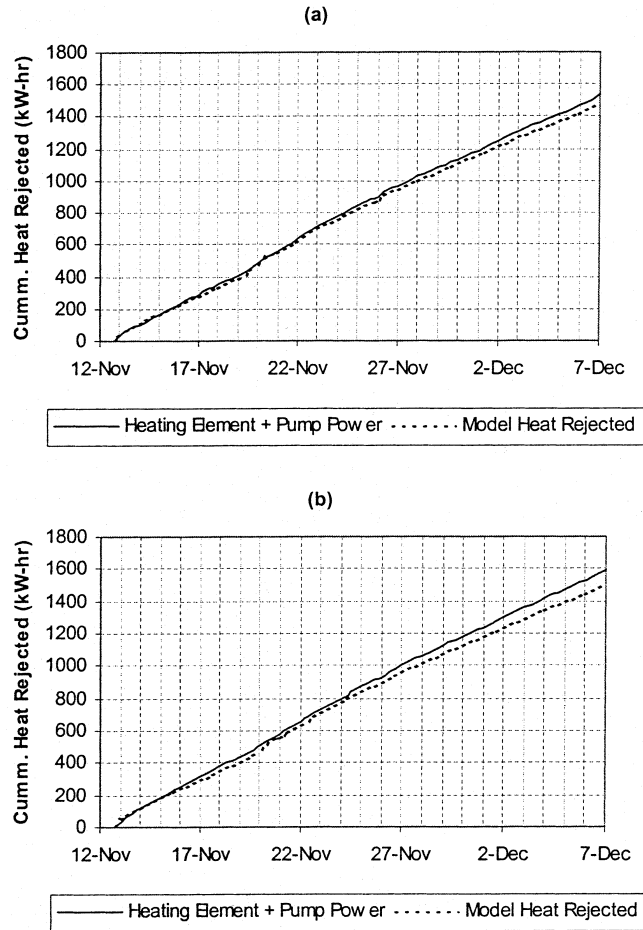


Figure 7 Comparison of observed and simulated heat rejected to the (a) 2 ft (0.61 m) deep pond and (b) 3.5 ft (1.07 m) deep pond.

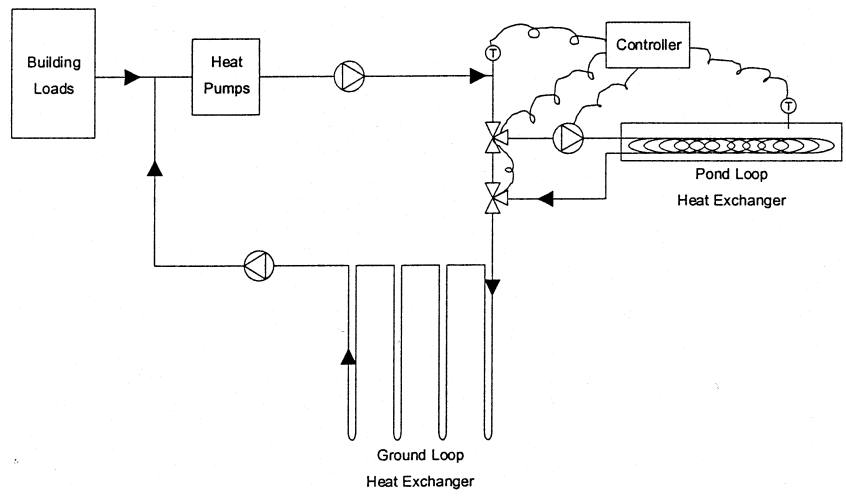


Figure 8 System schematic for the example model of a GSHP system with a shallow pond supplemental heat rejector.

deeper pond has slightly larger differences between modeled and observed fluid return temperatures. The error is small, however, and is probably acceptable for purposes of simulating hybrid GSHP systems; even a 2°F (1.11°C) error in return fluid temperature from the pond will cause only a slight difference in modeled heat pump performance.

A review of the plots in Figure 7 shows that the modeled cumulative heat rejected compares well to the measured heating element and pump power input. At the end of the 25-day test period, the percent difference between the cumulative simulated heat rejected and the cumulative measured heat rejected is -2.95% for the 2 ft deep (0.61 m) pond and -5.20% for the 3.5 ft (1.07 m) deep pond. These discrepancies may be due partly to heat losses from the pond's supply/return pipes to the ground and to the atmosphere in the equipment building.

Model Application

To illustrate the applicability of the model as well as the viability of using shallow ponds as supplemental heat rejecters in GSHP systems, a model of a hypothetical GSHP system was constructed in the TRNSYS modeling environment. A simplified system schematic is shown in Figure 8. Each of the component models is described briefly below.

The building is not modeled explicitly in this application. The hourly building thermal loads are precomputed using a proprietary building energy analysis program and are read from a file and passed to the heat pump subroutines. The building is an actual four-story, 45,000 ft² (4181 m²) office building located in Tulsa, Oklahoma, and is highly cooling-dominated. The building thermal loads are shown in Figure 9.

A simple water-to-air heat pump model was developed for this and other GSHP system simulations. Inputs to the model include sensible and latent building loads, entering fluid temperature, and fluid mass flow rate. The model uses quadratic curve-fit equations to manufacturer's catalog data to compute the heat of rejection in cooling mode, heat of absorption in heating mode, and the heat pump power consumption. Outputs provided by the model include exiting fluid temperature, power consumption, and fluid mass flow rate. In this application, one heat pump component model handles the heating load and a second heat pump component model handles the cooling load.

The ground-loop heat exchanger model used in this application is that described by Yavuzturk and Spitler (1999), which is based partly on the work of Eskilson (1987), who developed "long time step" (monthly) response factors for vertical ground-coupled U-tube heat exchangers. The model of Yavuzturk and Spitler (1999) extends the work of Eskilson (1987) to hourly or less (short time step) time intervals. The development of the short-time step response factors are based on an analytically validated, transient two-dimensional implicit finite volume model (Yavuzturk et al. 1999) that simulates the heat transfer over a vertical U-tube ground heat exchanger. In this application, the modeled borehole field consisted of one hundred 250 ft (76.2 m) deep boreholes

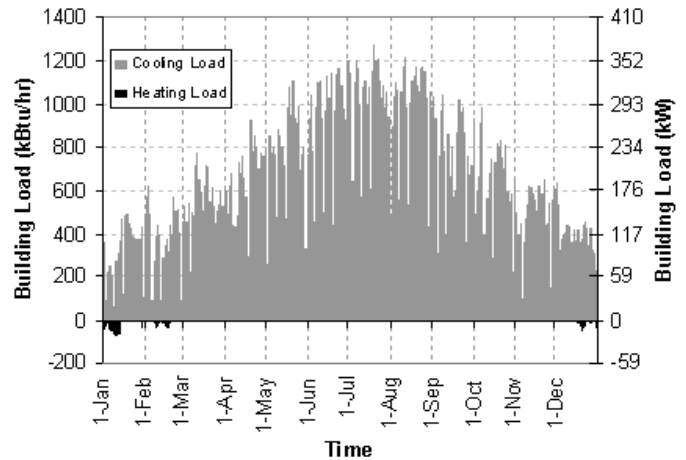


Figure 9 Building thermal loads for the example building in Tulsa, Oklahoma. Cooling loads are shown as positive values, indicating heat to be rejected to the GSHP system; heating loads are shown as negative values, indicating heat to be extracted from the GSHP system.

arranged in a 10 × 10 square pattern. The total system flow rate was 270 gpm (61.36 m³/h). Representative thermal properties of sedimentary rock were chosen.

Models for ancillary components, such as pumps, t-pieces, flow diverters, and the differential controller, are described by SEL (1997). The control strategy used to activate the circulating pump to the pond was chosen somewhat arbitrarily by using the temperature difference between the pond and the exiting fluid temperature from the heat pumps. When this temperature difference exceeds 9°F (5°C), the circulating pump to the pond is energized and heat will be rejected to the pond. During these times of heat rejection to the pond, flow is diverted to the pond so that each heat exchanger coil in the pond receives 4 gpm (0.909 m³/h) of water. The properties of each heat exchanger coil in the example model are the same as those described in the experimental procedure. Hourly input weather data for the pond model were taken from a typical meteorological year (TMY) record for Tulsa, Oklahoma.

The model was run for two cases for a duration of three years with a time step of one hour. The first case was the GSHP system with no pond and the second case was the GSHP system with the pond. Hourly heat pump entering water temperatures are shown in Figure 10 for both cases.

A review of the data presented in Figure 10 shows the advantages of using a pond supplemental heat rejecter. Assuming that a maximum heat pump entering water temperature of 100°F (37.78°C) is desirable, the system without the pond would fail during the second year of operation. In fact, based on the results of a ground-loop heat exchanger sizing program (Spitler et al. 1996), the boreholes of a 10 × 10 square pattern would need to be approximately 400 ft (121.9 m) deep

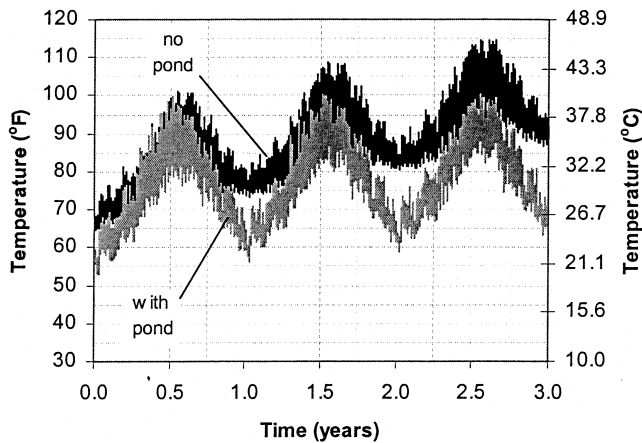


Figure 10 Entering heat pump water temperatures for the example GSHP system simulation with no pond and with a 2 ft (0.6096 m) deep, 6000 ft² (557.4 m²) pond.

to accommodate the cooling-dominated loads of this building for 20 years of operation. Such a system would be eliminated from consideration early on in the design phase because of excessive first cost.

Using the TRNSYS model as a design tool, the size of the pond's supplemental heat rejecter was determined under the assumption that the 10 × 10 borehole field could not be feasibly deeper than 250 ft (76.2 m). The heat pump entering water temperatures for the GSHP system with the pond shown in Figure 10 were produced by simulating a 2 ft (0.61 m) deep, 6000 ft² (557 m²) pond with 50 slinky heat exchanger coils. A summary of pond performance is given in Table 1. By adding the pond's supplemental heat rejecter in this example, the depth of the borehole field could be decreased by approximately 35%.

Ultimately, the economics of using a pond for supplemental heat rejection will determine whether or not the technology may be applied in practice. A detailed economic analysis is beyond the scope of this paper, but a simple economic analysis may be helpful in determining whether or not further research into the idea is warranted. Specifically, there are two questions that we will attempt to answer – first, is the cost of the pond heat rejection system significantly less than the savings in the

required borehole depth; second, is the cost of the pond heat rejection system competitive with more traditional heat rejection equipment, such as a cooling tower?

First, the anticipated savings in the ground-loop heat exchanger cost may be determined on a cost per foot basis. The savings in total borehole length are 15,000 ft (4572 m). Drilling costs vary, but a typical number, reported by Kavanaugh (1998), which includes drilling, grouting, and pipe, is \$6.00/ft (\$20/m). Thus, the total savings in ground loop heat exchanger cost is approximately \$90,000.

The cost of the pond may vary widely depending on site conditions, whether or not a pond might be present for other reasons, such as drainage retention, and whether or not real estate has to be purchased in order to incorporate the pond into the system. For purposes of our analysis, we assume that the pond must be excavated on reasonably level ground but that the excavated soil may be disposed of on site. Furthermore, we assume the real estate is already available and does not represent an extra cost. Obviously, if this is not the case, the economics may be significantly different. Excavation costs are taken from Ogershok and Phillips (1999). The pond requires approximately 444 yd³ (340 m³) of soil to be moved. Using a 120 HP (90 kW) bulldozer with an excavation rate of 25 yd³/h (19 m³/h) would require two days of bulldozer rental plus pickup and delivery charges at a total of \$1250. Operator costs would be approximately \$500. The HDPE pipe, in bulk, would cost about \$0.20/ft (\$0.66/m) (Schoen 1999), and with 50 slinkies, each 500 ft (152 m) long, the total cost for piping would be \$5000. Each slinky will require about half an hour to fabricate and half an hour to install. At \$15/h, the labor cost for fabricating and installing the slinkies is about \$750. Pond liners, which may or may not be required, cost anywhere from \$0.55 to \$1.12 per square foot (\$5.92 to \$12.05 per square meter). Taking an intermediate value of \$0.75 per square foot (\$8.07 per square meter), the total cost for the pond liner, if required, would be about \$4500. Also, the additional cost of piping and controls for the pond heat rejecter may be assumed roughly equivalent to the cost of piping and controls for a supplemental cooling tower. Extrapolating from the numbers given by Kavanaugh (1998), the piping and controls cost approximately \$3600. The total cost for the pond would then be \$15,600. For this case, the \$90,000 savings are well worth the \$15,600 cost of the pond. Of course, as already noted, the economics will be highly site specific.

TABLE 1
Summary of Pond Performance for Example GSHP System Simulation

Year	Hours ON	Average Pond Temperature		Heat Pump Maximum Entering Fluid Temperature		Heat Rejected	
		(°F)	(°C)	(°F)	(°C)	(kBtu)	(MJ)
1	3937	74.79	23.77	99.95	37.75	1,618,224	1,706,903
2	4873	76.37	24.65	100.29	37.94	2,160,080	2,278,452
3	5324	77.52	25.29	100.18	37.88	2,498,961	2,635,904

How does the cost of the pond compare to a cooling tower? An approximate answer may be determined by estimating the required cooling tower size. Looking at the third year of operation, the pond has a peak summertime heat rejection rate of approximately 616,000 Btu/h (180.6 kW). This would roughly correspond to a cooling tower appropriate for 41 ton (144 kW) air-conditioning capacity. In order to maintain the closed-loop nature of the ground-source heat pump, a plate frame heat exchanger would also be required. Kavanaugh (1998) reports on complete costs for three different sizes of cooling tower and plate frame heat exchanger, including the equipment, installation, controls, and piping. Extrapolating downward to a 41 ton (144 kW) unit, the estimated cost of the cooling tower, plate frame heat exchanger, installation, controls, and piping is \$16,367. Thus, the cost of the pond may be very similar to the cost of the cooling tower, assuming the real estate is not an extra cost. Of course, if a retention pond is already available or no pond liner is needed, the pond may be significantly lower in cost.

So, the answers to the questions raised above are that the pond does appear to make sense, at least in this application, and it appears to be competitive with a cooling tower and plate frame heat exchanger used in the same application. Necessarily, this is a very rough economic analysis. There are a large number of parameters fixed for this application that may be significantly different in other applications. These include location/climate, building load profile, ground thermal properties, ground loop design parameters, such as peak allowable entering fluid temperature, etc. All of these parameters will affect the economics. Also, maintenance costs, which may be expected to be significantly higher for the cooling tower (Kavanaugh 1998), have not been included here. Furthermore, no attempt has been made here at optimizing either the pond design or its control strategy. Limited attempts to optimize the design and control strategies for a cooling tower-based hybrid ground-source heat pump system (Yavuzturk 1999) have resulted in significant first cost and operating cost savings over previously reported systems. It is one of the purposes of the simulation tools presented in this paper to allow such an investigation to be performed for hybrid ground-source heat pump systems that utilize ponds for supplemental heat rejection.

CONCLUSIONS AND RECOMMENDATIONS

A design and simulation tool for modeling the performance of a shallow pond as a supplemental heat rejecter in ground-source heat pump systems has been developed. The model has been developed in the TRNSYS modeling environment (SEL 1997) and can be coupled to other GSHP system component models for short time step (hourly or less) system analyses. The model has been validated by comparing simulation results to experimental data.

The model accounts for several natural heat transfer mechanisms within a surface water body plus convective heat transfer due to a closed-loop heat exchanger coil. The heat

transfer fluid is assumed to be carried by a series of pipes in the form of bundled spools, or slinky coils. Environmental heat transfer mechanisms that are simulated by the model include solar radiation heat gain, heat and mass transfer due to evaporation, convective heat transfer to the atmosphere, thermal or long-wave radiant heat transfer, conductive heat transfer to the surrounding soil or fill material, and groundwater discharge contributions. The solution scheme involves a lumped-capacitance approach, and the resulting first-order differential equation describing the overall energy balance on the pond is solved numerically. Some outputs provided by the model include average pond temperature, exiting fluid temperature, and heat rejected to the pond.

An example application has been presented to demonstrate the use of the model as well as the viability of the use of shallow ponds as supplemental heat rejecters in GSHP systems. Through this example, it is shown that the size of ground-loop heat exchangers can be significantly decreased by incorporating a shallow pond into the GSHP system.

The potential exists for significantly increasing the performance of shallow ponds used as supplemental heat rejecters in GSHP systems. Further research is suggested in the following areas:

- Optimization of the design procedure and control strategy. Hybrid ground-source heat pump systems have many degrees of freedom; there are trade-offs between the reduction in size of the ground-loop heat exchanger, the size of the pond, and the control strategy. To more fully understand this, additional research using the simulation techniques developed in this paper is needed. This research would also take into account the economic costs and benefits that we have not investigated.
- Additional validation of the model, using data from a working system, would be useful.
- Extension of the model to cover deep ponds for situations where an existing pond or lake is available.
- The use of spray fountains and other aeration devices in the pond to enhance pond cooling.
- The impact of pipe configuration within the pond on the overall system performance.

ACKNOWLEDGMENTS

This work was supported by the U.S. Department of Energy through contract awards DE-FG48-97R810627 and DE-FG48-94R689416. Support by the Department of Energy does not constitute endorsement of the views expressed in this article.

NOMENCLATURE

Symbols

- α = thermal diffusivity, ft²/h (m²/s)
 ϵ = emissivity coefficient (-)

θ	= angle of incidence of sun's rays (radians)
ρ	= density, lb/ft ³ (kg/m ³)
ρ'	= reflectance of pond surface (-)
σ	= Stephan-Boltzmann constant = 0.1714×10^{-8} Btu/h·ft ² ·°R ⁴ (5.67×10^{-8} W/m ² ·K ⁴)
A	= area, ft ² (m ²)
c_p	= specific heat capacity, Btu/lb _m ·°F (J/kg·°C)
D	= binary diffusion coefficient, ft ² /h (m ² /s)
d	= depth, ft (m)
ff	= fouling factor, ft ² ·°F/h·Btu (m ² ·°C/W)
h	= heat or mass transfer coefficient, Btu/h·ft ² ·°F (W/m ² ·°C)
I	= solar radiant flux on horizontal, Btu/h·ft ² (W/m ²)
i	= hydraulic gradient, ft/ft (m/m)
K	= hydraulic conductivity, ft/s (m/s)
k	= thermal conductivity, Btu/h·ft·°F (W/m·°C)
L	= characteristic length, ft (m)
Le	= Lewis number (-)
\dot{m}''	= mass flux, lb _m /h·ft ² (kg/s·m ²)
\dot{m}	= mass flow rate, lb _m /h (kg/s)
N	= quantity (-)
Nu	= Nusselt number (-)
P	= perimeter, ft (m)
Pr	= Prandtl number (-)
Q	= volumetric flow rate, ft ³ /s (m ³ /s)
q	= heat transfer rate, Btu/h (W)
R	= thermal resistance, ft ² ·°F/h·Btu (m ² ·°C/W)
Ra	= Rayleigh number (-)
Re	= Reynolds number (-)
T	= temperature, °F (°C)
t	= time (s)
U	= overall heat transfer coefficient, Btu/h·ft ² ·°F (W/m ² ·°C)
V	= volume, ft ³ (m ³)
w	= humidity ratio, lb _m water/lb _m dry air (kg water/kg dry air)

Subscripts and Superscripts

AB	= transfer from material A (water) to material B (air)
b	= beam radiation
c	= convection
$circuit$	= flow circuit or spool
d	= diffuse radiation; diffusion
fg	= latent heat of vaporization
$fluid$	= heat exchange fluid
i	= pipe inside
in	= inlet
o	= pipe outside

out	= outlet
r	= thermal radiation; refraction
$surf$	= surface
w	= water

REFERENCES

- ASHRAE. 1995a. *1995 ASHRAE Handbook—HVAC Applications*. Atlanta: American Society of Heating, Refrigerating and Air-Conditioning Engineers, Inc.
- ASHRAE. 1995b. *Commercial/institutional ground-source heat pump engineering manual*. Atlanta: American Society of Heating, Refrigerating and Air-Conditioning Engineers, Inc.
- ASHRAE. 1997. *1997 ASHRAE Handbook—Fundamentals*. Atlanta: American Society of Heating, Refrigerating and Air-Conditioning Engineers, Inc.
- Bliss, R.W. 1961. Atmospheric radiation near the surface of the ground. *Solar Energy* 5(103).
- Cantrell, J.M., and W.J. Wepfer. 1984. Shallow ponds for dissipation of building heat: A case study. *ASHRAE Transactions* 90(1): 239-246.
- CRC. 1980. *Handbook of chemistry and physics*, 61st edition. Cleveland, Ohio: Chemical Rubber Company, CRC Press.
- Chiasson, A.D. 1999. *Advances in modeling of ground-source heat pump systems*. Unpublished master's thesis, Oklahoma State University, Stillwater.
- Churchill, S.W., and H.H.S. Chu. 1975. Correlating equations for laminar and turbulent free convection from a horizontal cylinder. *International Journal of Heat and Mass Transfer* 18: 1049-1053.
- Dake, J.M.K., and D.R.F. Harleman. 1969. Thermal stratification in lakes: Analytical and laboratory studies. *Water Resources Research* 5(2): 484-495.
- Duffie, J.A., and W.A. Beckman. 1991. *Solar engineering of thermal processes*, 2d ed. New York: John Wiley & Sons.
- Elliot, R.L., F.V. Brock, M.L. Stone, and S.L. Sharp. 1994. Configuration decisions for an automated weather station network. *Applied Engineering in Agriculture* 10(1): 45-51.
- Eskilson, P. 1987. Thermal analysis of heat extraction boreholes. Doctoral thesis, University of Lund, Department of Mathematical Physics, Sweden.
- Hull, J.R., K.V. Liu, W.T. Sha, J. Kamal, and C.E. Nielsen. 1984. Dependence of ground heat losses upon solar pond size and perimeter insulation—Calculated and experimental results. *Solar Energy* 33(1): 25-33.
- Incropera, F.P., and D.P. DeWitt. 1996. *Introduction to heat transfer*, 3d ed. New York: John Wiley & Sons.
- Irvine, T.F., Jr., and P.E. Liley. 1984. *Steam and gas tables with computer equations*. Academic Press, Inc.
- Jobson, H. 1973. The dissipation of excess heat from water systems. *Journal of the Power Division, Proceedings of*

- the American Society of Civil Engineers* 99(P01): 89-103.
- Kavanaugh, S.P., and K. Rafferty. 1997. *Ground-source heat pumps. Design of geothermal systems for commercial and institutional buildings*. Atlanta: American Society of Heating, Refrigerating and Air-Conditioning Engineers, Inc.
- Kavanaugh, S.P. 1998. A design method for hybrid ground source heat pumps. *ASHRAE Transactions* 104(2): 691-698.
- Kishore, V.V.N., and V. Joshi. 1984. A practical collector efficiency equation for nonconvecting solar ponds. *Solar Energy* 33(5): 391-395.
- SEL. 1997. 1997. *TRNSYS, A Transient Systems Simulation Program, User's Manual, Version 14.2*. Solar Energy Laboratory, University of Wisconsin-Madison.
- McAdams, W.H. 1954. *Heat transmission*, 3d ed. McGraw-Hill Book Company.
- Newell, T.A. 1984. Solar ponds—Alternate energy systems. *Military Engineer, Journal of the Society of American Military Engineers*, March-April, 492: 110-113.
- Ogershok, D., and D. Phillips. 1999. *National construction estimator*, 47th ed. Carlsbad: Craftsman Book Company.
- Pezent, M.C., and S.P. Kavanaugh. 1990. Development and verification of a thermal model of lakes used with water source heat pumps. *ASHRAE Transactions* 96(1): 574-582.
- Raphael, J.M. 1962. Prediction of temperatures in rivers. *Journal of the Power Division, Proceedings of the American Society of Civil Engineers*, July, 88(P02): 157-181.
- Rubin, H., B.A. Benedict, and S. Bachu. 1984. Modeling the performance of a solar pond as a source of thermal energy. *Solar Energy* 32(6): 771-778.
- Schoen, F. 1999. Personal communication.
- Spencer, J.W. 1971. Fourier series representation of the position of the sun. *Search* 2(5).
- Spitler, J.D., C. Marshall, R. Delahoussaye, and M. Manicham. 1996. *Users Guide of GLHEPRO*. Stillwater, Okla.: School of Mechanical and Aerospace Engineering, Oklahoma State University.
- Srinivasan, J., and A. Guha. 1987. The effect of reflectivity on the performance of a solar pond. *Solar Energy* 39(4): 361-367.
- Wadivkar, O. 1997. *An experimental and numerical study of the thermal properties of a bridge deck de-icing system*. Unpublished master's thesis, Oklahoma State University, Stillwater.
- Yavuzturk, C., and J.D. Spitler. 1999. A short time step response factor model for vertical ground-loop heat exchangers. *ASHRAE Transactions*, 105(2): 475-485.
- Yavuzturk, C., J. D. Spitler, and S. J. Rees. 1999. A transient two-dimensional finite volume model for the simulation of vertical U-tube ground heat exchangers. *ASHRAE Transactions* 105(2): 527-540.
- Yavuzturk, C. 1999. Modeling of vertical ground loop heat exchangers for ground source heat pump systems. Ph.D. thesis, School of Mechanical and Aerospace Engineering, Oklahoma State University.

This paper has been downloaded from the Building and Environmental Thermal Systems Research Group at Oklahoma State University (www.hvac.okstate.edu)

The correct citation for the paper is:

Chiasson, A.D., J.D. Spitler, S.J. Rees, M.D. Smith. 2000. A Model For Simulating The Performance Of A Shallow Pond As A Supplemental Heat Rejecter With Closed-Loop Ground-Source Heat Pump Systems. ASHRAE Transactions. 106(2):107-121.

Reprinted by permission from ASHRAE Transactions (Vol. #106 Part 2, pp. 107-121).
© 2000 American Society of Heating, Refrigerating and Air-Conditioning Engineers, Inc.